Version of Record: https://www.sciencedirect.com/science/article/pii/S0169555X18300035
Manuscript_ec0c78e5347a1c48fface90dd5b0eeac

The evolution of a colluvial hollow to a fluvial channel with periodic steps following two transformational disturbances: A wildfire and a historic flood

F. K. Rengers[a,1,*], L. A. McGuire[b], B. A. Ebel[c], G. E. Tucker[d]

[a] *Landslide Hazards Program, U.S. Geological Survey, Golden, CO, USA*
[b] *University of Arizona, Tucson, AZ, USA*
[c] *National Research Program, U.S. Geological Survey, Denver, CO, USA*
[d] *CIRES and Department of Geological Sciences, University of Colorado, Boulder, CO, USA*

Abstract

The transition of a colluvial hollow to a fluvial channel with discrete steps was observed after two landscape-scale disturbances. The first disturbance, a high-severity wildfire, changed the catchment hydrology to favor overland flow, which incised a colluvial hollow, creating a channel in the same location. This incised channel became armored with cobbles and boulders following repeated post-wildfire overland flow events. Three years after the fire, a record rainstorm produced regional flooding and generated sufficient fluvial erosion and sorting to produce a fluvial channel with periodically spaced steps. An analysis of the step spacing shows that after the flood, newly formed steps retained a similar spacing to the topographic roughness spacing in the original colluvial hollow (prior to channelization). This suggests that despite a distinct change in channel form roughness and bedform morphology,

*Corresponding author
Email address: frengers@usgs.gov (F. K. Rengers)

the endogenous roughness periodicity was conserved. Variations in sediment erodibility helped to create the emergent steps as the largest particles ($>D_{84}$) remained immobile, becoming step features, and downstream soil was easily winnowed away.
Keywords: colluvial hollow, wildfire, erosion, steps

1. Introduction

Understanding the geomorphic response following extreme landscape disturbances requires the ability to predict where and how sediment will be eroded from a landscape. A primary location for sediment storage between disturbance events, and thus a prime location for erosion, is the colluvial hollow landform; defined as a convergent hillslope feature located between sideslopes and hillslope noses (*Hack and Goodlett*, 1960; *Hack*, 1965). Because of their inherent convergent topography, hollows fill with colluvial sediment over time (*Reneau et al.*, 1990). Fluvial channels begin where colluvial hollows end, and the exact point of channel initiation fluctuates with time as a result of the competition between colluvial processes and fluvial processes (*Montgomery and Dietrich*, 1989; *Dietrich and Dunne*, 1993; *Perron et al.*, 2008a). In some geographic settings, colluvial hollows are evacuated via landslides with material traveling downstream as debris flows (*Reneau et al.*, 1990). This leads to a temporary extension of the fluvial network. In drainage basins that are not prone to landslides, the primary opportunity for fluvial extension into colluvial hollows occurs when water runoff or soil piping is sufficiently large to begin channel incision (e.g., *Horton*, 1945; *Schumm*, 1956; *Dunne*, 1980; *Montgomery and Dietrich*, 1989). *Glock* (1931, p. 479) conceptualized

this process in anthropomorphic terms, 'The growing streams reach out into the territory bequeathed them and take possession of their inheritance by means of headward elongation ...' Consequently, in the absence of landslides, the main opportunity for extension of the surface water network is through conversion of colluvial hollows into first-order fluvial channels.

The hydrologic conditions that lead to colluvial hollow erosion via overland flow are rare, especially in forested settings. In forests, the typical infiltration capacity of soils greatly exceeds the intensity range of most frequent rainfall events (e.g., *Dunne*, 1978; *Anderson*, 1990; *Shakesby and Doerr*, 2006). Consequently, extreme rainfall events are often required to generate overland flow sufficient to incise colluvial hollows in forested environments. Alternatively, overland flow can also be produced in forests by changing the infiltration capacity rather than the rainfall intensity. Soil-altering events such as wildfire can lead to a threshold change in soil hydrologic processes resulting in overland flow on parts of a formerly vegetated landscape that would typically only produce subsurface flow (*Morris and Moses*, 1987; *Benavides-Solorio and MacDonald*, 2001; *Shakesby and Doerr*, 2006; *Ebel et al.*, 2012a). Recently burned landscapes, unaccustomed to overland flow, will often erode rapidly during moderate rainstorms; and colluvial hollows commonly experience incision as they transition into 'rejuvenated gullies' (*Hyde et al.*, 2007). Moreover, newly formed channels frequently develop a series of steps or headcuts (e.g., *Leopold and Miller*, 1956; *Blong*, 1970; *Montgomery and Dietrich*, 1989; *Reid*, 1989; *Cannon et al.*, 2003).

Unlike step-pools, which are features formed via sediment reorganization and a preferential sorting of sediment to form steps (e.g., *Abrahams et al.*,

1995; *Chin*, 1999; *Curran*, 2007; *Comiti et al.*, 2009), the steps observed in incising colluvial hollows are more akin to headcuts, eroding into the colluvial sediment or bedrock (Fig. 1). New in-channel steps form when water plunges over an obstacle, or a hydraulic jump occurs on an erodible bed, and the downstream bed develops a plunge pool that deepens until it eventually reaches a dynamic equilibrium depth (e.g., *Farhoudi and Smith*, 1985; *Bennett*, 1999; *Gioia and Bombardelli*, 2005). Steps focus water flow to enhance hydraulic scouring of sediment and downstream fluvial incision (e.g., *Lapotre and Lamb*, 2015). At the brink of each step, flow accelerates, which imposes increased shear stresses in the downstream plunge pool (*Stein and Julien*, 1993; *Haviv et al.*, 2006). Moreover, the impinging jet can undercut the step or scour the plunge pool, creating a hot-spot for sediment transport in plunge pools downstream of steps (e.g., *Stein and Julien*, 1993; *Flores-Cervantes et al.*, 2006). In-channel steps may play a crucial role in developing debris flows. For example, *Kean et al.* (2013) demonstrated how channels with alternating high and low gradient sections (i.e., similar to alternating steps and plunge pools) can promote debris flow initiation. The low gradient areas preferentially store sediment transported as bedload during storms until the developing deposit becomes unstable as a mass and fails, creating a debris flow surge. The increased sediment transport at steps also likely contributes to sediment bulking (*Cannon et al.*, 2003), a process wherein debris flows form when sediment derived from a series of discrete pulses of erosion combines to raise the sediment concentration to a level above that of normal water flow.

Herein we seek to understand step formation in response to landscape

disturbances by using terrestrial LiDAR to explore the emergence of steps within a colluvial hollow after a natural experiment formed by two rare hydrologic disturbances, a wildfire (>30-year recurrence interval; *Sherriff and Veblen*, 2007) and a rainstorm (>1000-year recurrence interval; *Gochis et al.*, 2015). This builds upon several recent studies that have documented the conversion of colluvial hollows (i.e., convergent hillslopes) to gullies (i.e., channelized fluvial reaches) during runoff events following wildfire (*Cannon et al.*, 2003; *Moody and Kinner*, 2006; *Hyde et al.*, 2007; *Gabet and Bookter*, 2008; *Hyde et al.*, 2014; *Rengers et al.*, 2016). Because steps are a dominant roughness element when present and because of the potential implications for sediment transport and debris flow initiation, we focus on providing a mechanistic explanation for step development and step spacing at our study site.

During colluvial hollow incision, we hypothesize that the spacing of new channel steps are not independent of the initial surface roughness, as might be expected in a bed solely shaped by hydrodynamics. Rather, the spacing of steps in the newly formed channel are inherited from the surface roughness spacing that existed in the colluvial hollow (which presumably formed over hundreds to thousands of years). This hypothesis is based on field observations in burned areas of step formation near resistant materials such as tree roots and large rocks (*Cannon et al.*, 2003). In this case, newly incised steps would not be wholly independent of the initial colluvial hollow topography. An alternative hypothesis is that steps form at a natural wavelength, independent of channel erodibility, because of the hydrodynamic interaction between flowing water and an erodible bed (e.g., *Bryan et al.*, 1990; *Parker and Izumi*, 2000).

We used observed changes in channel topography from the terrestrial LiDAR to look for evidence supporting these hypotheses at our study sites. Because colluvial hollows sit at the interface between hillslopes and channels and are an important storage location for sediment between extreme events, knowledge of the step formation processes that accompany the hollow-to-channel transition is needed for understanding the response of drainage networks to disturbance events.

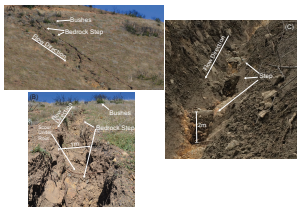

Fig. 1: Examples of step development in different settings after recent wildfire events. (A) View of newly created gully with steps after the Silverado, CA wildfire. (B) close-up view of the gully in A, where bedrock can be observed at steps and the position of a root crossing the gully indicates the depth of scour. As a reference point, the bushes labeled in A and B represent the same features and are about 5 m wide. (C) View of steps formed in preexisting colluvium after the First Creek wildfire near Lake Chelan, WA. Each step is about 2 m high. (Photo credit: F. Rengers)

2. Study site

The study site was burned by the 2010 Fourmile Canyon fire and is located in the foothills of the Colorado Front Range, 12 km west of Boulder, CO (Fig. 2). The local rock formation underlying the site is the Boulder Creek Granodiorite (*Gable*, 1980). Soil developing from decomposition of the underlying bedrock results in a gravelly sandy loam (part of the Allens Park

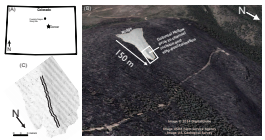

Fig. 2: (A) Site location in Colorado, USA. (B) Oblique view of study site, with gray-shaded relief polygon delineating the study area. White box indicates the inset C. (C) Shaded relief LiDAR from 7 October 2010 prior to channel incision. Two black lines indicate two longitudinal profiles bounding the stream (23 additional profiles are obtained between these two bounding profiles). Flow direction of the channel is generally north. The center of the site is located at: 40°1'54"N, 105°24'13"W.

member of the Fern Cliff-Allens Park-Rock outcrop complex (*Moreland and Moreland*, 1975)). Mean annual precipitation at the site is ∼500 mm, which typically falls as snow in the winter between approximately November and March and as rain during the rest of the year (*Ebel et al.*, 2012a).

Vegetation before the fire was typical of a north-facing montane ecosystem (*Marr*, 1961), with dominant tree species of aspen (*Populus tremuloides*), Rocky Mountain Douglas-fir (*Pseudotsuga menziesii* subspecies *glauca*), and Limber pine (*Pinus flexilis*) (*Peet*, 1981). During the wildfire, litter-duff was fully converted to ash leaving the forest floor almost entirely devoid of organic matter. Trees at the site were killed and charcoalified but remained standing. Throughout the study period we observed little toppling by either the dead tree trunks or branches. Consequently, minimal woody debris was available to either block erosion on the forest floor or contribute to the formation of bedforms in the channel. Shrubs and ground vegetation recovered within two years of the wildfire. This likely helped to reduce erosion in most hillslope areas; however, the main channel remained largely devoid of any vegetation.

2.1. Prior LiDAR collection and observed geomorphic evolution

Terrestrial laser scanning (TLS) data were collected during five separate field campaigns following the Fourmile Canyon wildfire (*Rengers et al.*, 2016), and a sixth LiDAR survey was conducted focusing on the channelized portion of the burn area after a historic rainfall event from 9–17 September 2013 (Table 1). The first LiDAR survey was obtained over a two-day period of 6–7 October 2010, 24 days following the wildfire. There was no appreciable rainfall at the field site prior to the first survey. A second survey was obtained (14–18 October 2010) after a low-intensity rain/snow precipitation event on 12 October 2010. The next survey took place on 11 – 12 July 2011, following several rainstorms in June and July 2011 (max 5-minute rainfall intensity: 80 mm/h) that caused erosion of the colluvial hollow, creating a fluvial channel and subsequent armoring (in the channel and on hillslopes *Rengers et al.*, 2016). A survey on 15 July 2011 was conducted after rainstorms that started on the evening of 12 July and continued through 13–14 July 2011 (max 5-minute rainfall intensity: 77 mm/h). Channel armoring from previous storms repressed further channelized erosion; consequently, relatively little sediment erosion was observed in the channel between 12 and 15 July 2011, despite the high intensity of the rainstorm (*Rengers et al.*, 2016). A survey was conducted on 1–2 May 2012 to capture the change from thunderstorms and snowmelt runoff in the 2011–2012 winter season (max 5-minute rainfall intensity: 30 mm/h). Channel erosion between these surveys was relatively limited, perhaps reflecting the dearth of high-intensity rainfall events (*Rengers et al.*, 2016). A final LiDAR survey (the focus of this study) was conducted on 8 October 2013 to capture geomorphic change following the extreme rainfall

from 9 to17 September 2013 (max 5-minute rainfall intensity: 41 mm/h). The characteristics and rarity of the 2013 storm are summarized by *Gochis et al.* (2015), and the extraordinary hydrologic and geomorphologic response are described in recent publications (*Coe et al.*, 2014; *Ebel et al.*, 2015, 2016; *Moody*, 2016).

Tab. 1

LiDAR surveys after the wildfire with hydrologic, roughness, and geomorphic metrics

Name	Date	Days after the wildfire	Peak flow before LiDAR survey (L/s)	H-Parameter	Slope (°)
Survey 1	7 October 2010	24	negligible	0.55	20.06
Survey 2	18 October 2010	35	1.2[a]	0.5	20.09
Survey 3	12 July 2011	302	46[a]	0.35	20.03
Survey 4	15 July 2011	305	n/a[b]	0.35	19.96
Survey 5	1 May 2012	596	29[a]	0.2	20.05
Survey 6	8 October 2013	1121	57[c]	0.25	20.14

[a] Measured with a modified Parshall flume (see *Rengers et al.* (2016)

[b] Unmeasured because flume filled with sediment

[c] Indirect estimate (see *Moody* (2016))

3. Methods

3.1. LiDAR collection

For all surveys, we used a tripod-mounted Riegl VZ-400 LiDAR scanner with ±5 mm accuracy and ±3 mm precision (*Riegl*, 2012). The scanner was

set up at several different scan positions for each survey (typically between 9 and 14 separate positions), and ∼100 reflective targets were used as control points on tree trunks (near the base of the trees for stability). A TopCon differential GPS was used to georeference four benchmarks on rock outcrops at the corners of the site. Further details about the LiDAR survey methods can be found in *Rengers et al.* (2016). The data from the LiDAR surveys used in this study can be found in (*Rengers*, 2017).

3.2. LiDAR processing

The TLS survey data were used to explore geomorphic change following several data processing steps. Point clouds from individual scan locations in the TLS survey were aligned using RiSCAN Pro version 2.1, and a root mean squared error (RMSE) tolerance of 0.005 m with a minimum of five common targets was used to select the best alignment. The point clouds from each survey were imported to ArcGIS, and a triangular irregular network (TIN) was used to create a continuous surface. The TIN was interpolated to a digital elevation model (DEM) with a grid cell size of 5 cm. The channel portion of the DEM was identified using a change in curvature to identify the channel edges. Using the first survey DEM, a flow accumulation grid was calculated with the D-infinity method in TauDEM (version 5.1.1; *Tarboton*, 1997), and the main channel thalweg was selected as the grid cells with the highest flow accumulation.

The channel width was 125 cm approximately, and we extracted 25 parallel longitudinal profiles along the channel with the identified channel thalweg in the middle of the extracted profiles (Fig. 2C). The channel slope was determined by dividing the vertical drop over a constant horizontal length

interval (0.5 m), and then each of these subreach slope angles were averaged. This method of slope calculation was used rather than a simple backward difference in order to prevent the average slope angle from being strongly influenced by a few high slope angle values associated with near-vertical portions of the channel.

3.3. Step observations

Erosion between LiDAR surveys can make it difficult to directly compare longitudinal profiles and to observe bedform changes. Consequently, each longitudinal profile was detrended to remove the influence of the topographic slope using the 'zero-crossing analysis' method (*Richards*, 1976) and cross section averaged (using 25 profiles for each survey) (Fig. 3). In this method, a linear regression model is fit to the bed profile, and then the longitudinal profile is subtracted from the regression profile. In order to observe the development of new steps in the longitudinal profile after the September 2013 rainstorm, we specifically examined changes to the thalweg between May 2012 and October 2013, when the channel transitioned from an ephemeral fluvial channel with defined banks and large cobbles (a cascade channel reach; *Montgomery and Buffington*, 1997) to a fluvial channel with alternating step and plunge pool bedforms. The May 2012 profile was detrended using the 'zero-crossing analysis' method (*Richards*, 1976), and the October 2013 longitudinal profile was then subtracted from the May 2012 slope regression model. This approach reveals the relative changes in the thalweg as steps and plunge pools developed during the 2013 flood (Fig. 4).

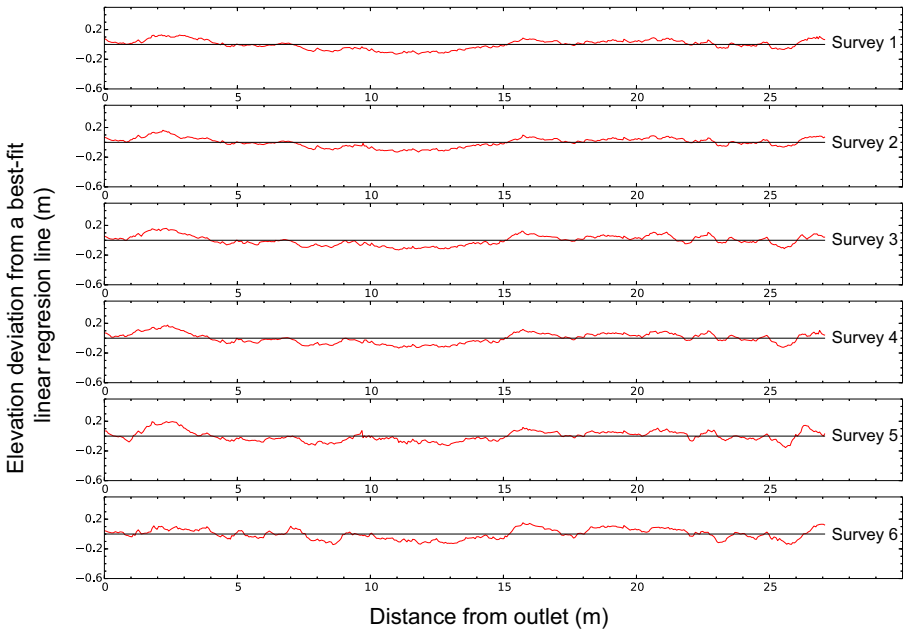

Fig. 3: The detrended longitudinal profile from each LiDAR survey that was cross section averaged using 25 profiles. A linear-regression line was fit to each profile, and the real-world elevation was subtracted in order to remove the slope effect.

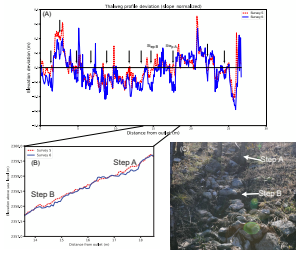

Fig. 4: (A) Detrended longitudinal profiles of the thalweg for May 2012 and October 2013 with new step-plunge pool locations are identified (by eye) with a black arrow. (B) Longitudinal profile for May 2012 and October 2013, without detrending and enlarged to allow observation of two new step-plunge pool locations. (C) Photo showing steps A and B, with step A partially obscured. (Photo credit: F. Rengers)

3.4. Spectral analysis

In order to explore how roughness spacing changed as the colluvial hollow transitioned to a fluvial channel with steps, we used Fourier analyses. In particular, the presence of periodic roughness within the channel was assessed using Fourier analyses of longitudinal profiles that were detrended (zero-crossing method) and cross section averaged. Each profile has a regular 5-cm spacing. Our approach closely follows that presented by *Perron et al.* (2008a) for using Fourier-based methods to quantify periodic patterns within topography, so we give only a brief outline of our methods here. First, a Hann window function is applied to each topographic transect, using the same technique as *Perron et al.* (2008b). The power spectrum of each transect is then approximated by using a discrete Fourier transform (DFT) to compute the DFT periodogram (Fig. 5A). Peaks in the DFT periodogram indicate that a periodicity, associated with a given frequency bin, is present in the topographic data. In addition, the topography of the longitudinal profiles changes over

time, and the power spectrum for each survey is expected to differ. Therefore, for a more direct comparison, we created a normalized power spectrum of each profile by dividing the power spectrum of the actual topography by the power spectrum of the randomly generated topography (Fig. 5B-G).

A statistical test of the significance of an observed normalized peak can be formulated by considering the null hypothesis that the peak occurred by chance. Letting $\chi_2^2(x)$ denote the value of the χ^2 cumulative distribution function with two degrees of freedom evaluated at x, the null hypothesis can be rejected for a given frequency f with a confidence level α if the spectral power at f (i.e., $P_\alpha(f)$) exceeds the following (*Perron et al.*, 2008b):

$$P_\alpha(f) > \frac{1}{2}\chi_2^2(1-\alpha)\bar{P}(f), \tag{1}$$

where $\bar{P}(f)$ denotes the background spectrum of the topography. The background spectrum can be thought of as a measure of the spectrum of the topographic surface if there were no concentration of variance into particular frequency bands. In this study, $\bar{P}(f)$ was determined for each topographic transect by comparing the spectrum associated with the actual topography data to spectra derived from randomly generated topography. Given an appropriate background spectrum, one can define a normalized spectral power by dividing the left side of Eq. (1) by the right-hand side. Whenever the normalized power is >1, the null hypothesis can be rejected.

The first step in determining a background spectrum is to generate random topography. We used the midpoint displacement algorithm (*Fournier et al.*, 1982) to create topographic transects having the same length and grid spacing as the actual data. This approach was originally developed to approximate

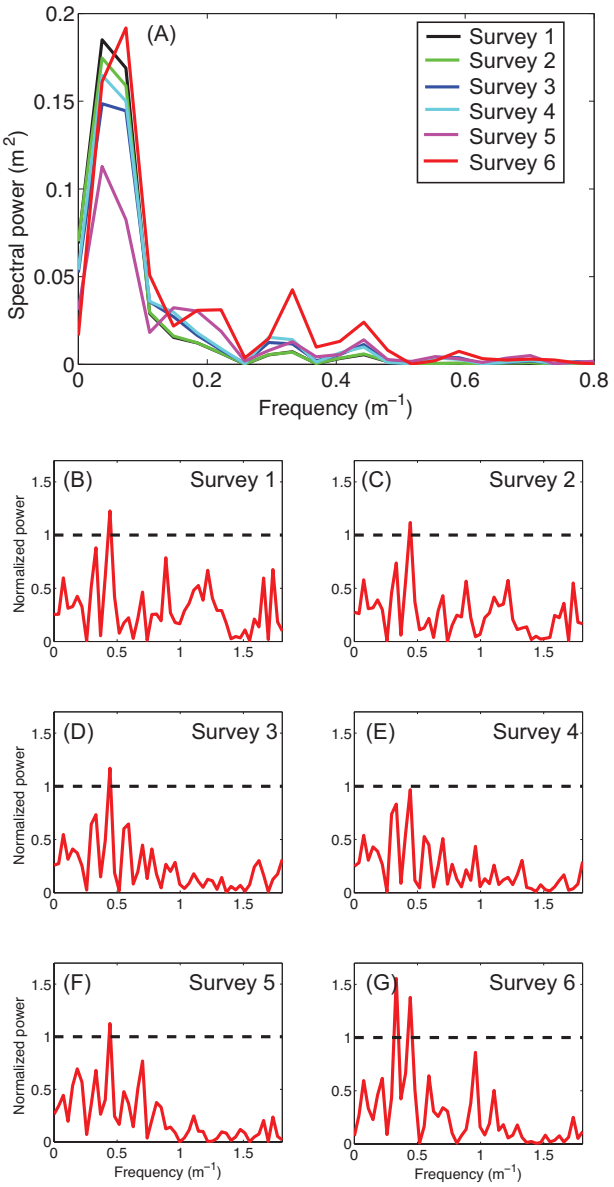

Fig. 5: (A) Power spectra for surveys 1–6 show a large increase in spectral power frequency bands near $f = 0.35\ m^{-1}$ and $f = 0.45\ m^{-1}$ following the most intense rainfall event (i.e., survey 6) (note the X-axis is clipped to remove low power values for frequencies >0.8). (B–G) Normalized power spectra for surveys 1–6. Each normalized power spectrum is obtained by dividing the ratio of $P_\alpha(f)$ to $\chi^2_2(1-\alpha)\bar{P}(f)$, as defined in section 3.4. The dashed line indicates the normalized power needed before the null hypothesis can be rejected with $\alpha = 0.05$.

fractional Brownian motion (fBm), and it is defined by an algorithm rather than a few simple equations. For this reason, we direct readers to Fournier et al. (1982) for a detailed explanation of the algorithm. However, one particular parameter is important to recognize. The roughness of the topography created through the midpoint displacement algorithm is controlled by a parameter H that varies from 0 to 1, and this H parameter determines the fractal dimension (*Fournier et al.*, 1982). The topography contains more high-frequency roughness elements when H is close to 0 and gets comparatively smooth (i.e., more of the spectral power is contained at lower frequencies) as H increases to 1. Inasmuch as a decrease in the spectral slope can be thought of as an increase in roughness, changes in the best-fit value of H can help to quantify changes in roughness. Examples of topography created using values of H = 0.25, H = 0.5, and H = 0.75 are illustrated in Fig. 6. By varying H, we can effectively change the roughness of the surface and consequently change properties of its Fourier spectrum (namely the spectral slope). Therefore, we created 10,000 random topographic transects for 19 evenly spaced values of H between 0.05 and 1 (creating a total of 190,000 total random transects). For each case, the spectra were computed and averaged. Then, for each of the six measured transects, we determined the best-fit value of H based on the optimal least squares fit between the actual and randomly generated spectra. Thus, if H=0.25 provided the best fit, then the background spectrum was set equal to the spectrum derived from topography generated using the midpoint displacement algorithm with H=0.25.

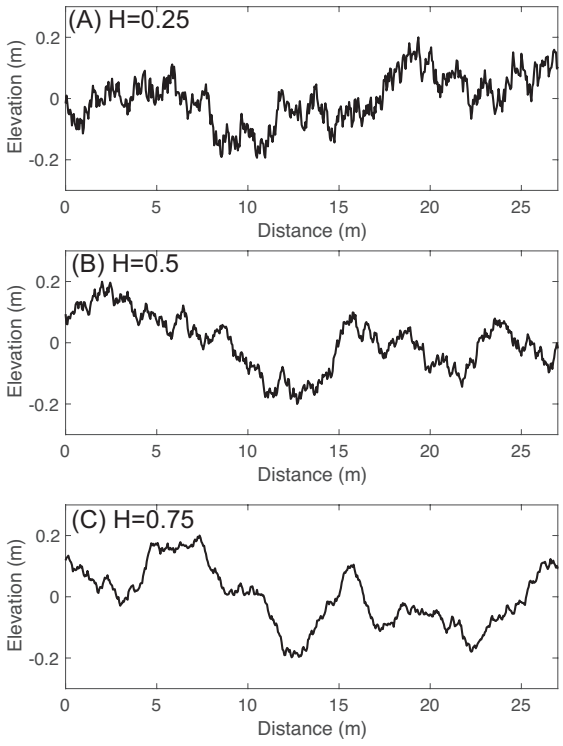

Fig. 6: Examples of topographic transects generated using the midpoint displacement algorithm with (A) $H = 0.25$, (B) $H = 0.5$, and (C) $H = 0.75$.

4. Results

The development of steps with downstream plunge pools was observed after the September 2013 rainstorm (Figs. 4 and 7), and plunge pool spacing was identified using the detrended profiles from the May 2012 and October 2013 surveys (Fig. 4A). The evolution of the topographic periodicity is clearly observed through the spectral analysis of each of the longitudinal profiles (Fig. 5). The DFT periodogram reveals that three prominent peaks are maintained in each of the longitudinal profiles (Fig. 5A). The first peak, near the frequency 0.05 m^{-1} or ∼20 m, approximates the length of the entire channel (25 m) and thus is an analysis artefact. Two additional peaks in the DFT periodogram occur near 0.35 m^{-1} and 0.45 m^{-1}, or 2.8 m and 2.2 m, respectively (Fig. 5A). Spectral peaks occur at these points in nearly all the surveys, and the magnitude of the spectral power is largest in the final survey after the September 2013 floods (Fig. 5A) following step formation (Fig. 7). Consequently, the new steps resulted in an amplification of the previously existing topographic periodicity, rather than a new frequency that was unrelated to the colluvial hollow topographic roughness (Fig. 5).

Fig. 7: A small reach within the study channel (6 m approximately) after the September 2013 flooding. The riser and tread portions of the steps are identified, and the lower riser arrow also shows the location of underlying bedrock. (Photo credit: F. Rengers)

The statistical significance analysis further confirms that the emergent steps after the flood retained a spacing similar to the extant periodicity prior

to the flood (Figs. 5B–G). The first and second LiDAR surveys demonstrate a single significant spectral power near 0.45 m^{-1} or 2.2 m (Figs. 5B–C), which is relatively low in overall magnitude (Fig. 5A). The third survey, where the most scour was observed prior to the September 2013 flood, shows a higher magnitude spectral power at 0.45 m^{-1} than the first two surveys (Fig. 5A). The fourth survey, just three days after the third survey shows a very similar spectral power to the third survey (Fig. 5A). Although the statistical significance of the spectral power at 0.45 m^{-1} is slightly reduced (significant at the $\alpha = 0.055$ level) in the data from the fourth survey, the pattern of the power spectra between the third and fourth surveys are nearly identical, peaking at 0.45 m^{-1} (Figs. 5D–E). The fifth survey, obtained more than 1 year after survey four, shows relatively little change in either the magnitude of the spectral power (Fig. 5A) or the pattern in the normalized spectral power (Fig. 5F), which matches observations suggesting little erosional channel change during that period (*Rengers et al.*, 2016). Finally, the sixth survey, following the September 2013 floods, demonstrates a statistically significant normalized spectral power near 0.35 and 0.45 m^{-1} (Fig. 5G), and a large jump in the overall magnitude increase in spectral power (Fig. 5A).

The field-observed changes in roughness can be seen quantitatively via a general decrease in the best-fit H parameter between surveys one and six (Table 1, Fig. 8). The H parameter is not a perfect metric for roughness because a cobble-boulder-dominated channel with steps can be composed of high-frequency (surface particles) and low-frequency (steps) roughness elements, which should result in a higher H parameter than a channel primarily dominated by surface particle roughness. For this reason we can also see

minor changes in the H parameter (e.g., the slight increase after the 2013 storm; Fig. 8). Nevertheless, the general trend of a decreasing H parameter since the wildfire is obvious (Fig. 8).

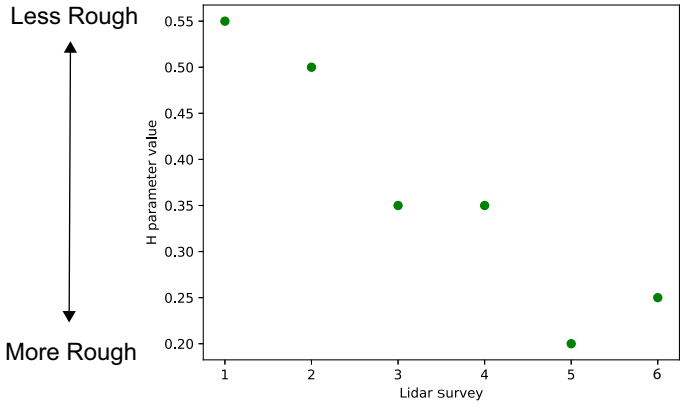

Fig. 8: The H parameter value from the channel for each LiDAR survey, where values of H=0 indicate a peak in high-frequency roughness and H=1 indicates smoother topography. The original colluvial hollow is relatively smooth and then becomes rougher over time as a fluvial channel is incised with a coarse cobble-boulder armor. The H parameter for the final channel morphology increases because periodic steps introduce a low-frequency periodicity that increases the H parameter.

5. Discussion

The observed changes in channel morphology reflect the combined hydrologic disturbances induced by a wildfire and a large flood event. At the beginning of the study, the channel matched the characteristics of a colluvial hollow; there were no definable banks, and the hollow graded directly into the adjacent hillslopes (see Fig. 9c and Fig. 12 in *Rengers et al.*, 2016). Moreover, none of the sediment in the channel indicated fluvial sorting or rounding. The

wildfire disturbance increased overland flow runoff by reducing the infiltration capacity of the soil, eliminating vegetation canopy interception and reducing surface cover and hydraulic roughness (*Ebel et al.*, 2012a,b; *Moody and Ebel*, 2012; *Ebel*, 2013). These changes substantially increased the propensity for overland flow relative to nearby unburned areas (*Ebel et al.*, 2012a), and the occurrence of overland flow led to substantial erosion in the channel (*Rengers et al.*, 2016). The first large thunderstorms following the wildfire (between surveys 2 and 3) created scour that converted the colluvial hollow to a cascade channel type. This post-wildfire erosion and channel incision resulted in the exhumation of large clasts throughout the channel (*Rengers et al.*, 2016), with the largest sizes equal to half the channel width (Fig. 7A). The change in channel roughness is evident in the decrease in the best-fit H parameter between surveys 2 and 3 (Table 1).

The second landscape disturbance, the September 2013 flood, was produced by infiltration-excess overland flow from the hillslopes (*Ebel et al.*, 2015, 2016). This flood converted the channel's morphologic regime type to one of alternating steps and plunge pools. Our spectral analyses suggest that, although step formation became more pronounced after the 2013 flood, an underlying periodicity existed in the colluvial hollow that was maintained during subsequent channel incision and step formation. A spectral peak at 0.45 m^{-1} was observed and statistically significant in most of the preflood surveys. Another spectral peak at 0.35 m^{-1} was also present in preflood surveys but not statistically significant until the flood erosion accentuated this peak in the final survey. These spectral peaks between 0.35 and 0.45 m^{-1} do not necessarily represent two different step spacings, more likely they

indicate that steps are spaced within the range of 0.35-0.45 m^{-1}. *Perron et al.* (2008b) observed that when assessing the significance of periodic topography, a distinguishing characteristic of true positive observations compared to false positives is the clustering of spectral peaks. Because these peaks are consistent and located in a relatively tight distance range throughout all of the observed topographic surveys (e.g. clustered), this provides strong evidence that the steps are periodically spaced between ∼2.2 and 2.8 m (Fig. 5). Moreover, step spacing occurs at ∼2 channel widths (assuming a channel width of ∼1.25 m), which falls within the range of periodic spacing (0.42-2.40) observed in step-pool systems (*Chin*, 2002).

Many of the new steps after the 2013 flood were formed by scouring sediment downstream of large in-place boulders or boulder clusters via plunge pool erosion (e.g., Fig. 7). There was little evidence of sediment reorganization to form new, in-place steps, rather the steps were exhumed as overlying sediment was eroded. The flood flow hydraulics were likely influenced by the preexisting roughness pattern, which created natural steep sections to accelerate water flow. The origin of the periodicity of large roughness elements within the original colluvial hollow is unknown. It is possible that a prior scour event could have formed steps and that the channel subsequently refilled with sediment over time. Whatever the primary cause of the inherent prefire roughness periodicity, this study shows that the roughness spacing prior to the flood (the alternating steep and low slopes in the unincised channel profile) was retained.

As the erodible channel bed developed steps to accommodate the applied flow, the average channel slope adjusted by $<0.2^{\circ}$ despite a large increase

in roughness (e.g., H parameter). This evolution supports analytical work suggesting that channels will tend to minimize changes to the channel slope, while maximizing sediment transport (*White et al.*, 1981). The formation of steps is also congruent with the theory of maximum friction factor, which posits that channels with adjustable boundaries will rearrange in a manner that maximizes the friction factor (*Davies and Sutherland*, 1983). This study builds on those observations by showing that despite an increase in friction via step formation, it is possible to retain the topographic periodicity inherent in the hollow that predated channelization.

5.1. Why step formation

Post-wildfire erosion incised a colluvial hollow to create a fluvial channel with a cobble-boulder bed. Why did the subsequent large flood result in a conversion from the rough bed to a channel with periodic steps? One explanation is the longer duration of the 2013 precipitation event, which lasted nearly a week. Although the exact duration of overland flow at the site is unknown, it was likely much longer than the post-wildfire convective thunderstorms, which only lasted for a few hours (see Table 2 in *Rengers et al.*, 2016), and therefore there was more time available for fluvial erosion.

To further explore why steps formed, we investigated the shear stress generated by the September 2013 flood. The peak unit discharge was at least 0.045 m^2/s, which was estimated by indirect flow estimates after the flood (*Moody*, 2016). The shear stress on the bed can be calculated as

$$\tau = \rho g R S \tag{2}$$

where ρ is water density = 1000 $kg\ m^{-3}$, g is gravitational acceleration = 9.81 ms^{-2}, R is the hydraulic radius averaged over eight cross sections = 0.075 m, and the channel slope is $\sim$20°. This results in a shear stress of 270 Pa, which is much higher than the measured shear stress threshold for soils at the site (for which the median-measured shear resistance was 17 Pa; *Moody and Nyman*, 2013). Consequently, the soil can be easily eroded from the channel. By contrast, the largest particles are not as easy to move. Consider the D_{84} particle size, which was 10 cm (*Moody*, 2016). We can calculate the dimensionless Shield's parameter for this size particle as

$$\tau^* = \frac{\tau}{(\rho_s - \rho)gD} \tag{3}$$

where ρ_s is the sediment density = 2650 $kg\ m^{-3}$, and $D = D_{84}$ = 0.1 m. This suggests that the τ^* is 0.17. In steep mountain streams, it has been shown that the critical shear stress increases with channel slope (*Lamb et al.*, 2008) and the percentage of morphologic drag on the particle. Using the critical shear stress curves suggested by *Lamb et al.* (2008) and a potential morphologic drag between 40–60%, the critical shear stress required for particle motion on this slope would be 0.2–0.23. Therefore, particles 10 cm and larger would not be moved, which coincides with field observations that these particles remained in place, forming steps. This leads us to interpret the emergence of quasi-periodic steps as resulting from scouring of relatively finer sediment between (and especially immediately downstream of) larger immobile clasts. This interpretation accounts for the enhancement of existing wavelengths, as boulders were present as roughness elements before the flood.

5.2. Geomorphic implications

We observed that two rare, high-magnitude changes to a landscape resulted in conversion of a colluvial channel to a fluvial channel with alternating steps and plunge pools. However, the underlying periodicity of the colluvial channel is retained during this conversion because the colluvial sediment within the hollow contained particles large enough to remain immobile during the high water flow. This suggests that in the future, as the forest recovers and sediment is transported back into the channel by hillslope processes, these hard points will remain in the landscape at approximately the same spacing, even if they are buried by finer material. Moreover, this observed step development may help to explain debris flow surges in watersheds after wildfire. If colluvial hollows have an underlying series of hard points that can be converted to alternating steps and plunge pools during high flow events, then this naturally sets up a series of 'sediment capacitors' that could potentially lead to debris flow surges (*Kean et al.*, 2013).

More generally, we attribute step formation at our study site to natural variations in channel erodibility, as fine sediment is eroded and boulders emerge to function as steps, which supports our hypothesis. While hydrodynamic conditions likely helped to influence step development, the preexisting periodicity within the channel suggests that steps would have formed at a similar spacing regardless of the specific hydraulic conditions within the developing channel, as long as there was sufficient shear stress to excavate fine sediment. The natural variations in erodibility and a relatively loose hydraulic condition (i.e., sufficient flow to erode fine sediment) help to explain step and plunge pool formation at our study site and to inform our understanding of why steps

are commonly observed in recently incised colluvial hollows (e.g., *Leopold and Miller*, 1956; *Blong*, 1970; *Montgomery and Dietrich*, 1989; *Reid*, 1989; *Cannon et al.*, 2003).

6. Conclusions

In this study, we document the formation of periodic channel steps in a location formerly occupied by a colluvial hollow. We found that the spacing associated with channel steps was inherited from a roughness length scale that existed within the colluvial hollow prior to either channelization or step formation. Two fluvial disturbances ultimately led to the conversion of the colluvial hollow to a channel with alternating steps and plunge pools. The first disturbance, a wildfire, created suitable hydrologic conditions to develop overland flow and channel incision, removing fine sediment from the colluvial hollow and forming definable channel banks. The second disturbance, a large flood, resulted in step formation. The steps had a similar undulatory topographic spacing to the roughness periodicity prior to channel incision. This suggests that although the channel transitioned from a colluvial hollow to step and plunge pool morphology, the roughness periodicity was nearly constant across this morphologic transition. Despite step formation, the average channel slope was relatively constant, suggesting that the bed preferentially adjusted through sediment export toward an increasingly stable slope configuration. Results also imply that step formation in colluvial hollows is determined primarily by spatial variations in erodibility and roughness rather than by the achievement of specific hydrodynamic conditions. The development of steps from preexisting roughness spacing has implications for debris flow

surges that need step-like topography in order to develop 'sediment capacitor' locations that allow sediment to build up and then release as a debris flow surge. Therefore, in future studies an analysis of preexisting topography may help reveal the penchant for a channel to develop debris flows.

7. Acknowledgements

We thank UNAVCO for use of their LiDAR system. John Moody and Jason Kean provided insightful initial reviews of the manuscript. We are especially grateful to two anonymous reviewers and the helpful style edits provided by Richard Marston. The data used in this paper are available in *Rengers* (2017). Any use of trade, firm, or product names is for descriptive purposes only and does not imply endorsement by the U.S. Government. Partial support was provided by the National Science Foundation (EAR-1331828 and -0952247).

Abrahams, A. D., G. Li, and J. F. Atkinson (1995), Step-pool streams: Adjustment to maximum flow resistance, *Water Resources Research*, *31*(10), 2593–2602.

Anderson, B. T. P., M. G. (1990), Subsurface runoff, in *Process Studies in Hillslope Hydrology*, edited by M. G. Anderson and T. P. Burt, pp. 365–400, Wiley, Chichester.

Benavides-Solorio, J., and L. MacDonald (2001), Post-fire runoff and erosion from simulated rainfall on small plots, Colorado Front Range, *Hydrological Processes*, *15*(15), 2931–2952.

Bennett, S. (1999), Effect of slope on the growth and migration of headcuts in rills, *Geomorphology*, *30*(3), 273–290.

Blong, R. (1970), The development of discontinuous gullies in a pumice catchment, *American Journal of Science*, *268*(4), 369–383.

Bryan, R., et al. (1990), Knickpoint evolution in rillwash, *Catena, Supplement*, (17), 111–132.

Cannon, S., J. Gartner, C. Parrett, and M. Parise (2003), Wildfire-related debris-flow generation through episodic progressive sediment-bulking processes, western USA, in *Debris-Flow Hazards Mitigation: Mechanics, Prediction, and Assessment, Proceedings of the Third International Conference on Debris-flow Hazards Mitigation, Millpress, Rotterdam*, pp. 71–82.

Chin, A. (1999), On the origin of step-pool sequences in mountain streams, *Geophysical Research Letters*, *26*(2), 231–234.

Chin, A. (2002), The periodic nature of step-pool mountain streams, *American Journal of Science*, *302*(2), 144–167.

Coe, J. A., J. W. Kean, J. W. Godt, R. L. Baum, E. S. Jones, D. J. Gochis, and G. S. Anderson (2014), New insights into debris-flow hazards from an extraordinary event in the Colorado Front Range, *GSA Today*, *24*(10).

Comiti, F., D. Cadol, and E. Wohl (2009), Flow regimes, bed morphology, and flow resistance in self-formed step-pool channels, *Water Resources Research*, *45*(4).

Curran, J. C. (2007), Step–pool formation models and associated step spacing, *Earth Surface Processes and Landforms*, *32*(11), 1611–1627.

Davies, T. R., and A. J. Sutherland (1983), Extremal hypotheses for river behavior, *Water Resources Research*, *19*(1), 141–148.

Dietrich, W., and T. Dunne (1993), The channel head, in *Channel Network Hydrology*, edited by K. Beven and M. J. Kirkby, pp. 175–219, Wiley: Chichester.

Dunne, T. (1978), Field studies of hillslope flow processes, in *Hillslope Hydrology*, edited by M. J. Kirkby, pp. 227–293, Wiley, Chichester.

Dunne, T. (1980), Formation and controls of channel networks, *Progress in Physical Geography*, *4*(2), 211–239.

Ebel, B. A. (2013), Wildfire and aspect effects on hydrologic states after the 2010 Fourmile Canyon Fire, *Vadose Zone Journal*, *12*(1), 1–19, doi:10.2136/vzj2012.0089.

Ebel, B., J. Moody, and D. Martin (2012a), Hydrologic conditions controlling runoff generation immediately after wildfire, *Water Resources Research*, *48*(3), W03,529, doi:10.1029/2011WR011470.

Ebel, B., E. Hinckley, and D. Martin (2012b), Soil-water dynamics and unsaturated storage during snowmelt following wildfire, *Hydrology and Earth System Sciences*, *16*(5), 1401—1417, doi:10.5194/hess-16-1401-2012.

Ebel, B. A., F. K. Rengers, and G. E. Tucker (2015), Aspect-dependent soil

saturation and insight into debris-flow initiation during extreme rainfall in the Colorado Front Range, *Geology*, *43*(8), 659–662.

Ebel, B. A., F. K. Rengers, and G. E. Tucker (2016), Observed and simulated hydrologic response for a first-order catchment during extreme rainfall 3 years after wildfire disturbance, *Water Resources Research*, *52*(12), 9367–9389.

Farhoudi, J., and K. V. Smith (1985), Local scour profiles downstream of hydraulic jump, *Journal of Hydraulic Research*, *23*(4), 343–358.

Flores-Cervantes, J., E. Istanbulluoglu, and R. Bras (2006), Development of gullies on the landscape: A model of headcut retreat resulting from plunge pool erosion, *Journal of Geophysical Research*, *111*(F1), F01,010, doi:10.1029/2004JF000226.

Fournier, A., D. Fussell, and L. Carpenter (1982), Computer rendering of stochastic models, *Communications of the ACM*, *25*(6), 371–384.

Gabet, E. J., and A. Bookter (2008), A morphometric analysis of gullies scoured by post-fire progressively bulked debris flows in southwest Montana, USA, *Geomorphology*, *96*(3), 298–309.

Gable, D. J. (1980), Geologic map of the Gold Hill quadrangle, Boulder County, Colorado, Geologic Quadrangle Map GQ-1525, scale 1:24,000, *Tech. rep.*, U.S. Geological Survey, Reston, VA.

Gioia, G., and F. A. Bombardelli (2005), Localized turbulent flows on scouring granular beds, *Physical Review Letters*, *95*(1), 014,501.

Glock, W. S. (1931), The development of drainage systems: A synoptic view, *Geographical Review*, *21*(3), 475–482.

Gochis, D., R. Schumacher, K. Friedrich, N. Doesken, M. Kelsch, J. Sun, K. Ikeda, D. Lindsey, A. Wood, B. Dolan, et al. (2015), The great colorado flood of september 2013, *Bulletin of the American Meteorological Society*, *96*(9), 1461–1487.

Hack, J. T. (1965), Geomorphology of the Shenandoah Valley, Virginia and West Virginia, and origin of the residual ore deposits, *Professional Paper 484*, U.S. Geological Survey.

Hack, J. T., and J. C. Goodlett (1960), Geomorphology and forest ecology of a mountain region in the central Appalachians, *Professional Paper 347*, U.S. Geological Survey.

Haviv, I., Y. Enzel, K. Whipple, E. Zilberman, J. Stone, A. Matmon, and L. Fifield (2006), Amplified erosion above waterfalls and oversteepened bedrock reaches, *Journal of Geophysical Research: Earth Surface*, *111*(F4).

Horton, R. E. (1945), Erosional development of streams and their drainage basins; hydrophysical approach to quantitative morphology, *Geological Society of America Bulletin*, *56*(3), 275–370.

Hyde, K., S. W. Woods, and J. Donahue (2007), Predicting gully rejuvenation after wildfire using remotely sensed burn severity data, *Geomorphology*, *86*(3), 496–511.

Hyde, K. D., A. C. Wilcox, K. Jencso, and S. Woods (2014), Effects

of vegetation disturbance by fire on channel initiation thresholds, *Geomorphology*, *214*, 84–96.

Kean, J. W., S. W. McCoy, G. E. Tucker, D. M. Staley, and J. A. Coe (2013), Runoff-generated debris flows: Observations and modeling of surge initiation, magnitude, and frequency, *Journal of Geophysical Research: Earth Surface*, *118*(4), 2190–2207.

Lamb, M. P., W. E. Dietrich, and J. G. Venditti (2008), Is the critical shields stress for incipient sediment motion dependent on channel-bed slope?, *Journal of Geophysical Research: Earth Surface*, *113*(F2).

Lapotre, M. G., and M. P. Lamb (2015), Hydraulics of floods upstream of horseshoe canyons and waterfalls, *Journal of Geophysical Research: Earth Surface*, *120*(7), 1227–1250.

Leopold, L. B., and J. P. Miller (1956), Ephemeral streams; hydraulic factors and their relation to the drainage net, *Professional Paper 282-A*, U.S. Geological Survey.

Marr, J. (1961), Ecosystems of the east slope of the Front Range in Colorado, *Series in Biology 8*, University of Colorado Studies.

Montgomery, D. R., and J. M. Buffington (1997), Channel-reach morphology in mountain drainage basins, *Geological Society of America Bulletin*, *109*(5), 596–611.

Montgomery, D., and W. Dietrich (1989), Source areas, drainage density, and channel initiation, *Water Resources Research*, *25*(8), 1907–1918.

Moody, J. A. (2016), Estimates of peak flood discharge for 21 sites in the Colorado Front Range in response to extreme rainfall in September 2013, *Scientific Investigations Report 2016-5003*, U.S. Geological Survey.

Moody, J., and B. Ebel (2012), Hyper-dry conditions provide new insights into the cause of extreme floods after wildfire, *Catena*, *93*, 58–63.

Moody, J., and P. Nyman (2013), Variations in soil detachment rates after wildfire as a function of soil depth, flow properties, and root properties, *Scientific Investigations Report 2012–5233*, U.S. Geological Survey.

Moody, J. A., and D. A. Kinner (2006), Spatial structures of stream and hillslope drainage networks following gully erosion after wildfire, *Earth Surface Processes and Landforms*, *31*(3), 319–337.

Moreland, D. C., and R. E. Moreland (1975), *Soil Survey of Boulder County Area, Colorado*, Natural Resources Conservation Service, United States Department of Agriculture, Washington, D.C.

Morris, S. E., and T. A. Moses (1987), Forest fire and the natural soil erosion regime in the Colorado Front Range, *Annals of the Association of American Geographers*, *77*(2), 245–254.

Parker, G., and N. Izumi (2000), Purely erosional cyclic and solitary steps created by flow over a cohesive bed, *Journal of Fluid Mechanics*, *419*, 203–238.

Peet, R. K. (1981), Forest vegetation of the Colorado Front Range, *Plant Ecology*, *45*(1), 3–75, doi:doi:10.1007/BF00240202.

Perron, J. T., W. E. Dietrich, and J. W. Kirchner (2008a), Controls on the spacing of first-order valleys, *Journal of Geophysical Research: Earth Surface*, *113*(F4).

Perron, J. T., J. W. Kirchner, and W. E. Dietrich (2008b), Spectral signatures of characteristic spatial scales and nonfractal structure in landscapes, *Journal of Geophysical Research: Earth Surface*, *113*(F4).

Reid, L. M. (1989), Channel incision by surface runoff in grassland catchments, Ph.D. thesis, University of Washington.

Reneau, S. L., W. E. Dietrich, D. J. Donahue, A. T. Jull, and M. Rubin (1990), Late Quaternary history of colluvial deposition and erosion in hollows, central California Coast Ranges, *Geological Society of America Bulletin*, *102*(7), 969–982.

Rengers, F. (2017), Fourmile Canyon Wildfire Longitudinal Profile Data: U.S. Geological Survey data release, https://doi.org/10.5066/F70P0XZ7.

Rengers, F. K., G. E. Tucker, J. A. Moody, and B. A. Ebel (2016), Illuminating wildfire erosion and deposition patterns with repeat terrestrial lidar, *Journal of Geophysical Research: Earth Surface*, pp. 588–608, doi:10.1002/2015JF003600, 2015JF003600.

Richards, K. (1976), The morphology of riffle-pool sequences, *Earth Surface Processes*, *1*(1), 71–88.

Riegl (2012), 3D Terrestrial Laser Scanner with Online Waveform Processing, *Tech. rep.*, Riegl Laser Measurement Systems.

Schumm, S. A. (1956), Evolution of drainage systems and slopes in badlands at Perth Amboy, New Jersey, *Geological Society of America Bulletin*, *67*(5), 597–646.

Shakesby, R., and S. Doerr (2006), Wildfire as a hydrological and geomorphological agent, *Earth-Science Reviews*, *74*(3), 269–307.

Sherriff, R. L., and T. T. Veblen (2007), A spatially-explicit reconstruction of historical fire occurrence in the ponderosa pine zone of the Colorado Front Range, *Ecosystems*, *10*(2), 311–323.

Stein, O., and P. Julien (1993), Criterion delineating the mode of headcut migration, *Journal of Hydraulic Engineering*, *119*(1), 37–50.

Tarboton, D. G. (1997), A new method for the determination of flow directions and upslope areas in grid digital elevation models, *Water Resources Research*, *33*(2), 309–319.

White, W., E. Paris, and R. Bettess (1981), River regime based on sediment transport concepts, *Tech. Rep. IT 201*, Hydraulics Research Station, Wallingford, England.

Graphical abstract

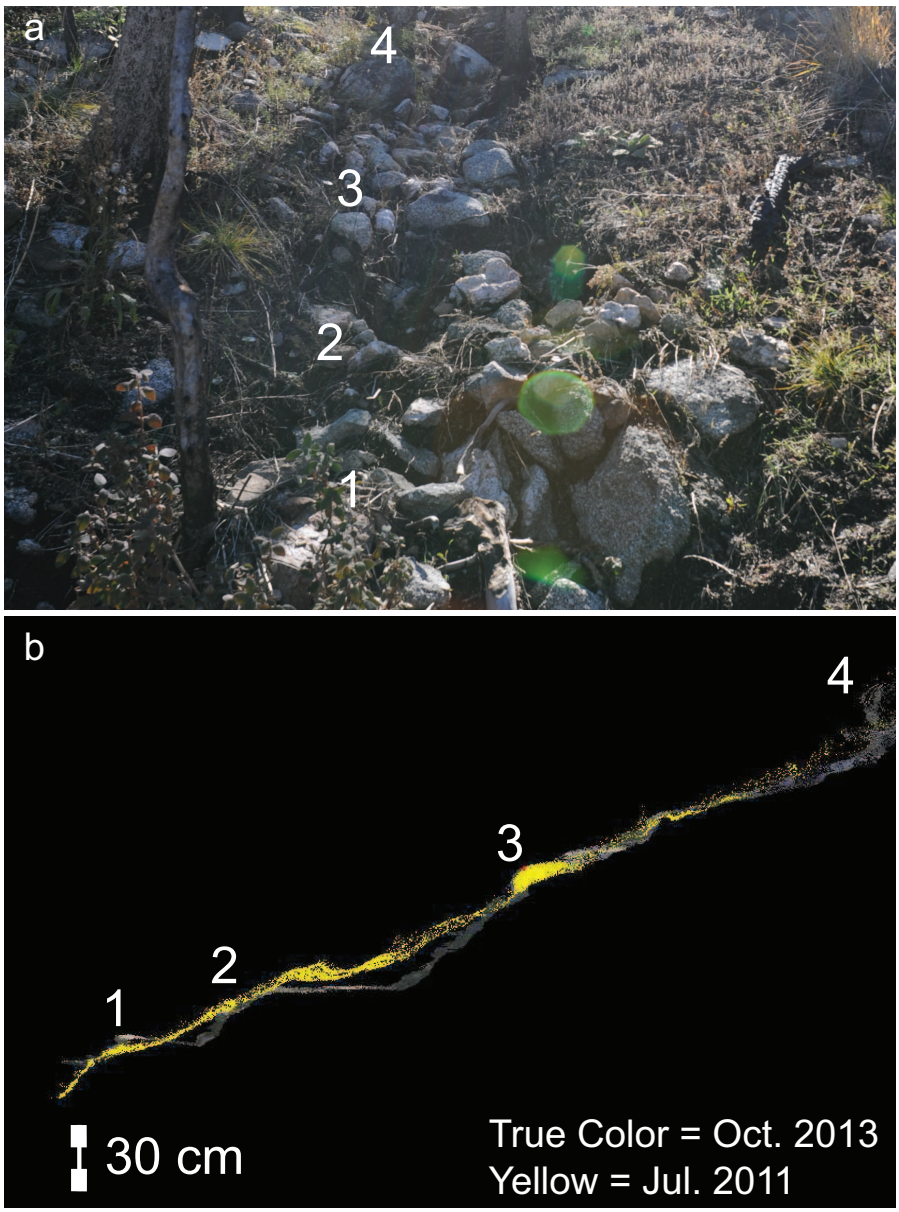

Abstract.pdf

Highlights

- Two hydrologic disturbances contributed to a geomorphic transition
- Alternating steps and plunge pools emerge from a colluvial hollow
- An inherent topographic roughness wavelength is maintained following disturbance events despite new bedforms